Experimental and Theoretical Study of the $R_3P^+-X^-$ Bond. Case of Betaines Derived from *N*-Iminophosphoranes and Alkyl Isocyanates

Pedro Molina,[†] Mateo Alajarín,[†] Carmen López Leonardo,[†] Rosa María Claramunt,[‡] M. de la Concepción Foces-Foces,[§] Félix Hernández Cano,[§] Javier Catalán,[∥] José Luis G. de Paz,[∥] and José Elguero*[,⊥]

Contribution from the Departamento de Química Orgánica, Universidad de Murcia, 30001 Murcia, Spain, Departamento de Química Orgánica, Universidad Nacional de Educación a Distancia, 28040 Madrid, Spain, U.E.I. de Cristalografía, Instituto de Química Física "Rocasolano", 28006 Madrid, Spain, Departamento de Química Física, Universidad Autónoma de Madrid, 28049 Madrid, Spain, and Instituto de Química Médica, CSIC, 28006 Madrid, Spain. *Received February 10, 1988*

Abstract: The synthesis of betaines **3** (**a**, R = Me; **b**, R = Et; **c**, R = nPr), bearing simultaneously a negative charge delocalized through an amidine system and a positive one in an iminium phosphorane moiety, is described. In solution, ^{1}H NMR reveals the existence of a chiral center, which results from the electrostatic interaction between a negatively charged nitrogen and a positively charged phosphorus. The crystal structures of **3a**·$CHCl_3$, **3a**·$^1/_2C_4H_8O_2$, and **3c**·$2CHCl_3$ have been determined. These structures, with a quasi-pentacoordinated phosphorus, are intermediate between the open-chain betaine and the ring-chain 1,2,4-phosphadiazetidine. 6-31G* theoretical calculations have been carried out on H_3PO, H_3PNH, $[H_3PNH_2]^+$, and H_3PCH_2. The existence in iminium phosphorane inner salts **3** of an empirical relationship between the rotation about the $[P\text{---}N]^+$ bond and the pyrimidalization of the nitrogen has been confirmed theoretically. Similarly, in methylenephosphoranes the "parallel" conformation has a planar CH_2, whereas a pyramidal CH_2 corresponds to the "perpendicular" conformation. Finally, the nature of the P–O bond in H_3PO has been established through the study of Foster and Boys' localized molecular orbitals.

We have reported[1] that the iminophosphorane derived from 4-amino-6-methyl-3-(methylthio)-5-oxo-4,5-dihydro-1,2,4-triazine **1** reacts with aromatic isocyanates to give the corresponding

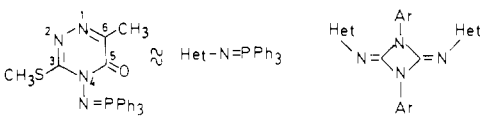

1

2

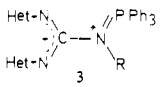

3

a, R = Me
b, R = Et
c, R = n-Pr

(*Z*,*Z*)-1,3-diaryl-2,4-bis[[6-methyl-3-(methylthio)-5-oxo-4,5-dihydro-1,2,4-triazin-4-yl]imino]-1,3-diazetidines (**2**). We describe here that the reaction of the same iminophosphorane with aliphatic isocyanates yields betaines **3**.

The originality of these structures prompted us to undertake their study. The molecular structures of **3a** and **3c** have been determined by X-ray analysis. In the case of **3a** this has been done with two different solvates, chloroform and dioxane, in order to establish that the structural characteristics are relatively independent of the crystal lattice.

Experimental Section

Syntheses. Melting points were recorded on a Kofler hot-stage apparatus and are uncorrected. Iminophosphorane **1** has already been described,[1] and alkyl isocyanates are commercial products.

General Procedure. To a solution of 6-methyl-3-(methylthio)-4-[(triphenylphosphoranylidene)amino]-5-oxo-4,5-dihydro-1,2,4-triazine (**1**) (0.5 g, 1.16 mmol) in dry benzene was added the corresponding alkyl isocyanate (0.58 mmol). The reaction mixture was stirred at room temperature for 1 h. The precipitated solid was collected by filtration and recrystallized from $CHCl_3$–petroleum ether.

3a: R = Me, mp 190 °C, yield 0.35 g (95%). Anal. Calcd for $C_{30}H_{30}N_9O_2S_2P$: C, 55.98; H, 4.70; N, 19.58. Found: C, 56.02; H, 4.63; N, 19.70. IR (Nujol): 1682 (s), 1540 (s), 1438 (m), 1331 (m), 1038 (s), 1291 (s), 1115 (m), 1076 (m), 996 (m), 855 (m), 753 (m), 719 (m), 691 (m) cm^{-1}.

3b: R = Et, mp 211–2 °C, yield 0.313 g (82%). Anal. Calcd for $C_{31}H_{32}N_9O_2S_2P$: C, 56.61; H, 4.90; N, 19.16. Found: C, 56.70; H, 4.85; N, 19.08. IR (Nujol): 1682 (vs), 1535 (s), 1438 (s), 1325 (s), 1308 (s), 1285 (vs), 1166 (m), 1115 (m), 1070 (m), 1013 (m), 999 (m), 755 (m), 731 (m), 686 (m) cm^{-1}.

3c: R = nPr, mp 193–4 °C, yield 0.275 g (71%). Anal. Calcd for $C_{32}H_{34}N_9O_2S_2P$: C, 57.21; H, 5.10; N, 18.76. Found: C, 57.16; H, 5.03; N, 18.84. IR (Nujol): 1682 (vs), 1540 (s), 1438 (m), 1325 (m), 1308 (s), 1285 (s), 1109 (m), 1070 (m), 1019 (m), 838 (m), 753 (m), 719 (m), 696 cm^{-1}.

4d: R = tBu, mp 102–3 °C, yield 0.055 g (19%). Anal. Calcd for $C_{10}H_{15}N_5OS$: C, 47.41; H, 5.97; N, 27.65. Found: C, 47.35; H, 6.08; N, 27.75. IR (Nujol): 2100 (vs), 1671 (vs), 1331 (m), 1240 (m), 1195 (m), 1070 (m), 963 (m), 747 (m) and 668 (m) cm^{-1}. MS (%): *m*/*z* 253 (9) [M] 240 (6), 239 (13), 238 (100) $[M - CH_3]^{\bullet+}$ 199, (5), 157 (7), 156 (57) (peaks below *m*/*z* 156 are not reported).

Crystal Structure Determinations. Suitable single crystals were obtained by slow evaporation from chloroform or dioxane.

Crystal data for **3a**·$CHCl_3$, **3a**·$^1/_2C_4H_8O_2$, and **3c**·$2CHCl_3$, are reported in Table I. Cell constants were obtained from least-squares fit of, respectively, 88, 84, and 67 reflections with $\theta \leq 45°$. During data collections, two standard reflections were monitored every 90 min, with no decay detected in **3a** solvates. Compound **3c**·$2CHCl_3$ was affected by air and light, so it was sealed into a Lindemann capillary. Standard reflections showed a 36% overall decay during this data collection. In the final stages of the refinement the parameters of the dioxane molecule in **3a**·$^1/_2C_4H_8O_2$ and five hydrogen atoms in **3c**·$2CHCl_3$ had to be kept fixed.

Calculations use the X-ray,[2] MULTAN,[3] and ORTEP[4] systems and the PLUTO package.[5] The absorption was corrected in an empirical way,[6] and the scattering factors were taken from ref 7. All computing was done on a Vax 11/750.

[†] Universidad de Murcia.
[‡] Universidad Nacional de Educación a Distancia.
[§] Instituto de Química Física "Rocasolano".
[∥] Universidad Autónoma de Madrid.
[⊥] Instituto de Química Médica.

(1) Molina, P.; Alajarin, M.; Saez, J. R.; Foces-Foces, M. C.; Hernández Cano, F.; Claramunt, R. M.; Elguero, J. *J. Chem. Soc., Perkin Trans. 1* **1986**, 2037.

(2) Stewart, J. M.; Machin, P. A.; Dickinson, C. W.; Ammon, H. L.; Heck, H.; Flack, H. *The X-Ray System*; Technical Report No. TR-446; Computer Science Center, University of Maryland: College Park, MD, 1976.

0002-7863/89/1511-0355$01.50/0

Table I. Crystal Analysis Parameters at Room Temperature with Cu Kα (λ = 1.5418 Å)

	3a·C	3a·D	3c
	A. Crystal Data		
chem formula	$C_{30}H_{30}N_9O_2S_2P\cdot CHCl_3$	$C_{30}H_{30}N_9O_2S_2P\cdot {}^1/_2C_4H_8O_2$	$C_{32}H_{34}N_9O_2S_2P\cdot (CHCl_3)_2$
FW	763.10	656.80	910.53
cryst color	yellow	yellow	colorless
cryst dimens, mm	0.10 × 0.27 × 0.33	0.23 × 0.17 × 0.10	0.20 × 0.30 × 0.50
space gp	$P2_1/n$	$P2_1/n$	$P\bar{1}$
a, Å	18.6258 (13)	23.7880 (9)	13.6288 (5)
b, Å	16.1925 (8)	9.3710 (2)	13.8194 (4)
c, Å	11.8443 (4)	15.3060 (5)	13.5059 (6)
α, deg	90	90	109.08 (1)
β, deg	101.91 (1)	94.79 (1)	90.43 (1)
γ, deg	90	90	65.17 (1)
V, Å^3	3495.3 (3)	3400.1 (2)	2156.8 (2)
ρ_{calc}, g·cm^{-3}	1.450	1.283	1.402
μ, cm^{-1}	43.29	17.58	53.20
	B. Intensity Measurements		
instrument	Philips PW 1100		
monochromator	graphite pyrolitic oriented, incident beam		
scan type	$\omega/2\theta$, bisecting geometry		
scan rate, min/reflcn	1		
scan width, deg	1.5		
max θ, deg	65		
abs corrcn	1.238–0.753	1.247–0.641	1.318–0.706
no. of indep data	5931	5752	7123
	C. Solution and Refinement		
solution	direct methods		
hydrogen atoms	found difference synthesis		
minimization function	$S \equiv \sum w(\|F_o\| - k\|F_c\|)^2$		
weights	empirical as to give no trends on $\langle s \rangle$ vs $\langle \|F_o\| \rangle$ and $\langle \sin\theta/\lambda \rangle$		
no. of reflcns obs ($3\sigma(I)$)	4593	3615	3814
no. of param	557	544	610
R, R_w[a]	0.054, 0.063	0.064, 0.066	0.092, 0.108
final largest shift/error	0.16	0.16	0.17
highest final ΔF peak, e·Å^{-3}	0.51	0.36	1.50

[a] $R \equiv \sum[|F_o| - k|F_c|]/\sum|F_o|$; $R_w \equiv [\sum w(|F_o| - k|F_c|)^2/\sum w|F_o|^2]^{1/2}$

Other Measurements. Infrared spectra were recorded as Nujol mulls on a Nicolet FT-5DX spectrophotometer. Nuclear magnetic resonance spectra were obtained on a Varian XL-300 with standard conditions (tetramethylsilane as internal reference for ^{1}H and ^{13}C NMR; 85% H_3PO_4 as external reference for ^{31}P NMR). Careful selective decoupling experiments were necessary to determine the coupling constants in ^{1}H NMR. Electron-impact mass spectra were measured on a Hewlett-Packard 5993C spectrometer at 70 eV.

Results and Discussion

Syntheses. Betaines **3** have been fully characterized (Table II). Presumably, the **1** → **3** conversion involves initial aza-Wittig reaction between iminophosphorane **1** and alkyl isocyanates to give the heteroarylmethylcarbodiimide **4** and triphenylphosphine oxide. The reaction stops at this stage when R = *tert*-butyl, **4d**. In the other cases, carbodiimide **4** reacts with the starting iminophosphorane **1** through a [2 + 2] cycloaddition to give a 1,2,4-phosphadiazetidine **5**. A ring-chain isomerism leads to betaine **3**.

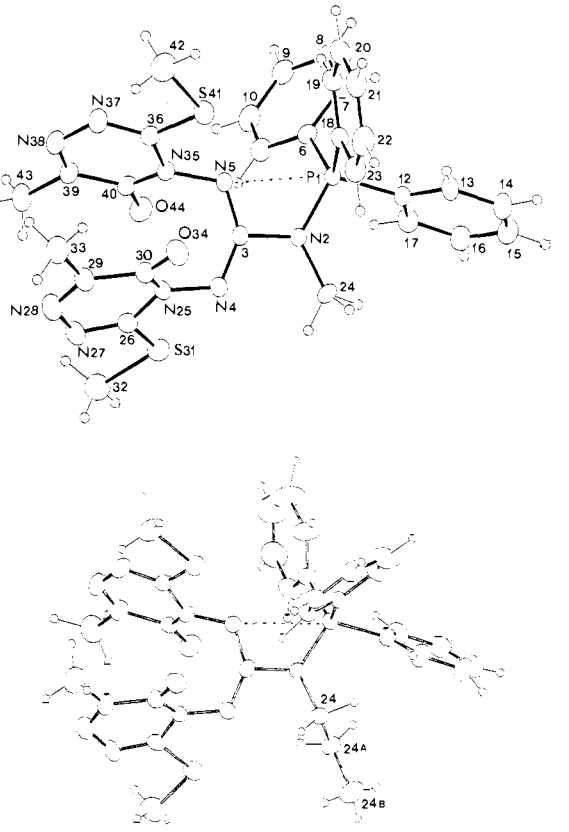

Figure 1. View of the molecule **3a**·$CHCl_3$ with the atomic numbering scheme for the **3a** components. For compound **3c**, the numbering for the carbon atoms of the *n*-propyl group is C24, C24A, and C24B.

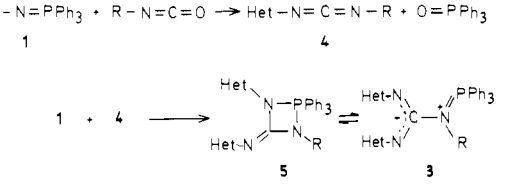

It has been described[8,9] that the reaction between iminophosphoranes and carbodiimides yields 1,2,4-phosphadiazetidines as intermediates, which undergo further reactions to give different products depending on the nature of the starting materials. In no case was the cycloadduct or the ring-open product isolated nor characterized. Literature iminophosphoranes have an Ar—N=PPh_3 structure;[8,9] thus, the different behavior we observe is probably due to the N–N bond in **1**.

The mass spectra (Table II) of betaines correspond to a retro [2 + 2] cycloaddition of the 1,2,4-phosphadiazetidine **5** with concomitant formation of the radical ions belonging to iminophosphorane **1** and carbodiimide **4**.

X-ray Crystallography

Description of Structures. Selected geometrical characteristics for compounds **3a**·$CHCl_3$ (**3a**·C), **3a**·$^1/_2C_4H_8O_2$ (**3a**·D), and **3c**·$2CHCl_3$ (**3c**) are given in Tables III and IV. The representative molecular structure, with the numbering scheme used for the three cases in the crystallographic analysis, is presented in Figure 1. The dioxane molecule adopts the expected ^oC_o chair conformation.[10]

(3) Main, P.; Fiske, S. J.; Hull, S. E.; Lessinger, L.; Germain, G.; Declerq, J. P.; Woolfson, M. M. *Multan 80 System*; University of York: England, 1980.
(4) Johnson, C. K. ORTEP; Report ORNL-3974, Oak Ridge National Laboratory: Oak Ridge, TN, 1965.
(5) Allen, F. H.; Bellard, S.; Brice, M. D.; Cartwright, B. A.; Doubleday, A.; Higgs, H.; Hummelink, T.; Hummelink-Peters, B. G.; Kennard, O.; Motherwell, W. D. S.; Rodgers, J. R.; Watson, D. G. *Acta Crystallogr.* **1979**, *B35*, 2331.
(6) Walker, N.; Stuart, D. *Acta Crystallogr.* **1983**, *A39*, 158.
(7) *International Tables for X-Ray Crystallography*; Kynoch: Birmingham, England, 1974; Vol. IV.
(8) Huisgen, R.; Wulff, J. *Chem. Ber.* **1969**, *102*, 1948.
(9) Bodeker, J.; Kockritz, P.; Courault, K. *Z. Chem.* **1979**, *19*, 59.
(10) Green, B. S.; Arad-Yellin, R.; Cohen, M. D. *Topics in Stereochemistry*; Wiley: New York, 1986; Vol. 16, p 131.

Table II. Spectroscopic Data

Compound **3a**

^{1}H NMR spectrum[a] (δ, J): 2.12 (s, C-Me); 2.32 (s, S-Me); 3.24 (d, N-Me, $^3J[^1H-^{31}P]$ = 11.0); 7.64 (m, 9 H), 7.86 (m, 6 H; Ph_3P)
^{13}C NMR spectrum[b] (δ, J): 14.56 (q, S-Me, ^1J = 142.0); 17.26 (q, C-Me, ^1J = 130.0); 160.43 (q, C3, ^3J = 4.5); 152.38 (q, C6, ^2J = 7.2); 148.88 (q, C5, ^3J = 3.5); 151.85 (d, C$^-$, $^3J[^{13}C-^{31}P]$ = 6.0); 36.62 (dq, N-Me, ^1J = 141.9, $^3J[^{13}C-^{31}P]$ = 4.5); 123.82 (m, C_{ipso}, $^1J[^{13}C-^{31}P]$ = 109.2); 133.7 (m, C_{ortho}, $^2J[^{13}C-^{31}P]$ = 10.4); 128.38 (m, C_{meta}, $^3J[^{13}C-^{31}P]$ = 13.6); 133.40 (m, C_{para}, $^4J[^{13}C-^{31}P]$ = 2.9)
^{31}P NMR spectrum[c] (δ): 35.40
Mass spectrum[d] (m/z): 432 (48%, [Het—N=PPh_3]$^{\bullet+}$); 211 (87%, [Het—NΔbdC=N—Me]$^{\bullet+}$

Compound **3b**

^{1}H NMR spectrum[a] (δ, J): 2.11 (s, C-Me); 2.32 (s, S-Me); 1.35 (t, N-CH_2*Me*); 3.39 (m, N-*CH_2*(*A*)-Me); 3.87 (m, N-*Ch_2*(*B*)-Me, (^3J[AMe] = ^3J[BMe] = 7.1; ^2J[AB] = −14.2 [J_{gem}]; $^3J[A^{31}P]$ = 14.2; $^3J[B^{31}P]$ = 16.7); 7.63 (m, 9 H), 7.87 (m, 6 H, Ph_3P)
^{13}C NMR spectrum[b] (δ, J): 14.63 (q, S-Me, ^1J = 142.0); 17.18 (q, C-Me, ^1J = 129.9); 160.47 (q, C3, ^3J = 4.3); 152.10 (q, C6, ^2J = 7.3); 148.67 (q, C5, ^3J = 3.5); 151.80 (d, C$^-$, $^3J[^{13}C-^{31}P]$ = 5.6); 16.19 (t, N-CH_2*Me*, ^1J = 127.6, ^2J = 3.3); 42.63 (m, N-*CH_2*Me, ^1J = 141.3, $^3J[^{13}C-^{31}P]$ = 3.5); 124.52 (m, C_{ipso}, $^1J[^{13}C-^{31}P]$ = 107.1); 133.68 (m, C_{ortho}, $^2J[^{13}C-^{31}P]$ = 11.7); 129.24 (m, C_{meta}, $^3J[^{13}C-^{31}P]$ = 12.9); 133.21 (m, C_{para}, $^4J[^{13}C-^{31}P]$ = 3.3)
^{31}P NMR spectrum[c] (δ): 34.70
Mass spectrum[d] (m/z): 432 (18%, [Het—N=PPh_3]$^{\bullet+}$) 225 (14%, [Het—N=C=N—Et]$^{\bullet+}$

Compound **3c**

^{1}H NMR spectrum[a] (δ, J): 2.12 (s, C-Me); 2.32 (s, S-Me); 0.64 (t, N-CH_2CH_2*Me*); 3.13 (m, N-*CH_2*(*A*)-CH_2Me); 3.74 (m, N-*CH_2*(*B*)-CH_2Me); 1.61 (m, N-CH_2-*CH_2*(*C*)-Me); 2.14 (m, N-CH_2-*CH_2*(*D*)-Me); ($^3J_{[AMe]}$ = $^3J_{[BMe]}$ = 7.3; $^2J_{[AB]}$ = −14.1 [J_{gem}]; $^3J_{[AC]}$ = 4.9 [J_{gauche}]; $^3J_{[AD]}$ = 11.1 [J_{trans}]; $^3J_{[BD]}$ = 4.6 [J_{gauche}]; $^3J_{[BC]}$ = 11.4 [J_{trans}]; $^2J_{[CD]}$ = −14.2 [J_{gem}]; $^3J_{[A^{31}P]}$ = 13.8; $^3J_{[B^{31}P]}$ = 17.2); 7.62 (m, 9 H), 7.87 (m, 6 H, Ph_3P)
^{13}C NMR spectrum[b] (δ, J): 14.56 (q, S-Me, ^1J = 141.6); 17.12 (q, C-Me, ^1J = 129.4); 160.63 (q, C3, ^3J = 3.3); 152.01 (q, C6, ^2J = 7.1); 148.66 (q, C5, ^3J = 3.0); 151.75 (d, C$^-$, $^3J[^{13}C-^{31}P]$ = 5.2); 10.83 (t, N-CH_2CH_2*Me*, ^1J = 126.2); 24.22 (m, N-CH_2*CH_2*Me, ^1J = 129.2, ^2J = 4.3); 48.92 (m, N-*CH_2*CH_2Me, ^1J = 140.2, $^3J[^{13}C-^{31}P]$ = 4.0); 124.32 (m, C_{ipso}, $^1J[^{13}C-^{31}P]$ = 107.5); 133.64 (m, C_{ortho}, $^2J[^{13}C-^{31}P]$ = 10.7); 129.20 (m, C_{meta}, $^3J[^{13}C-^{31}P]$ = 13.5); 133.12 (m, C_{para}, $^4J[^{13}C-^{31}P]$ = 2.5)
^{31}P NMR spectrum[c] (δ): 34.08
Mass spectrum[d] (m/z): 432 (5%, [Het—N=PPh_3]$^{\bullet+}$); 239 (9%, [Het—N=C=N—Pr]$^{\bullet+}$

[a] Recorded at 300 MHz in $CDCl_3$: s = singlet, d = doublet, t = triplet, m = multiplet; J values in Hz. [b] Recorded at 75 MHz in $CDCl_3$, unless indicated coupling constants refer to (^{1}H-^{13}C) couplings. [c] Recorded at 121 MHz in $CDCl_3$ (proton decoupled). [d] Recorded at 70 eV.

Table III. Selected Constitutional Characteristics

	3a·C	3a·D	3c		3a·C	3a·D	3c
			Distances, Å				
P1···N5	2.658 (3)	2.610 (4)	2.741 (7)	N28-C29	1.291 (6)	1.285 (8)	1.294 (17)
P1-N2	1.662 (3)	1.656 (4)	1.651 (8)	N38-C39	1.294 (5)	1.290 (8)	1.291 (19)
P1-C6	1.794 (3)	1.790 (5)	1.790 (9)	N4-N25	1.404 (4)	1.403 (5)	1.394 (10)
P1-C12	1.806 (3)	1.809 (5)	1.801 (11)	N5-N35	1.408 (4)	1.403 (5)	1.401 (8)
P1-C18	1.798 (4)	1.790 (5)	1.779 (10)	N27-N28	1.390 (5)	1.384 (7)	1.386 (18)
N2-C24	1.471 (5)	1.488 (7)	1.491 (12)	N37-N38	1.381 (5)	1.370 (7)	1.369 (14)
N2-C3	1.431 (4)	1.427 (6)	1.429 (10)	C26-S31	1.740 (4)	1.736 (5)	1.745 (13)
N25-C30	1.394 (5)	1.379 (7)	1.402 (14)	C36-S41	1.734 (4)	1.729 (6)	1.747 (10)
N35-C40	1.394 (5)	1.387 (7)	1.396 (11)	C32-S31	1.806 (7)	1.790 (8)	1.784 (14)
N25-C26	1.369 (6)	1.375 (6)	1.371 (14)	C42-S41	1.802 (7)	1.809 (9)	1.775 (18)
N35-C36	1.369 (5)	1.378 (7)	1.353 (16)	O34-C30	1.215 (5)	1.232 (6)	1.205 (12)
N4-C3	1.312 (5)	1.332 (6)	1.322 (14)	O44-C40	1.218 (4)	1.220 (6)	1.209 (14)
N5-C3	1.326 (4)	1.318 (6)	1.330 (14)	C29-C33	1.495 (7)	1.509 (9)	1.505 (23)
N27-C26	1.294 (5)	1.306 (7)	1.294 (12)	C39-C43	1.494 (7)	1.495 (10)	1.482 (19)
N37-C36	1.309 (5)	1.296 (7)	1.310 (12)				
			Angles, deg				
N2-P1-C6	115.6 (2)	114.9 (2)	112.6 (5)	C24-N2-P1	123.1 (2)	123.5 (3)	119.1 (6)
N2-P1-C12	104.8 (2)	104.5 (2)	106.4 (5)	N2-C3-N4	111.4 (3)	113.3 (4)	112.0 (8)
N2-P1-C18	111.9 (2)	113.5 (2)	111.9 (4)	N2-C3-N5	109.0 (3)	108.2 (4)	109.8 (8)
C6-P1-C12	102.7 (2)	103.4 (2)	107.0 (5)	N4-C3-N5	139.7 (3)	138.5 (5)	138.2 (9)
C6-P1-C18	113.5 (2)	112.2 (2)	112.3 (5)	C3-N4-N25	116.9 (3)	115.3 (4)	116.5 (8)
C12-P1-C18	107.1 (2)	107.2 (3)	106.1 (5)	C3-N5-N35	117.0 (3)	117.8 (4)	116.1 (8)
N5···P1-C12	161.8 (1)	162.2 (2)	157.2 (4)	C29-C30-N25	111.7 (3)	113.5 (5)	111.4 (9)
N5···P1-N2	57.2 (1)	57.8 (2)	55.4 (3)	C29-C30-O24	125.7 (4)	124.8 (5)	126.0 (9)
N5···P1-C6	85.3 (1)	84.2 (2)	73.0 (4)	N25-C30-O34	122.6 (3)	121.6 (5)	122.4 (9)
N5···P1-C18	83.9 (1)	84.0 (2)	94.4 (3)	C39-C40-N35	112.2 (3)	112.2 (5)	111.3 (8)
C3-N2-P1	118.3 (2)	117.4 (3)	121.0 (6)	C39-C40-O44	124.8 (3)	125.2 (5)	124.9 (9)
C3-N2-C24	118.2 (3)	118.5 (4)	117.5 (7)	N35-C40-O44	122.9 (3)	122.5 (5)	123.8 (9)

P1-N2-C3-N5 Pseudocycle. The three molecules conform around a central part, P1-N2-C3-N5, which is quite planar, the defined torsion angle being of −0.4 (4), 2.5 (5), and −8.7 (10)°, respectively, vs the free rotation the molecule could hold. Thus, there are contacts, of 2.658 (3), 2.610 (4), and 2.741 (7) Å, between N5 and P1, along a line that forms angles at P1 of about 57° with N2, 84° with either C6 or C18, and about 160° with C12 (see Table III and Figure 1). Around P1, C12 makes angles with N2, C6, and C18 of lower value than tetrahedral, while the other three angles around are greater. Within the achieved precision, P1-C12 is longer than the other P1-C(Ph) bonds.

Thus, it seems that the tetrahedron at P1 is distorted toward a bipyramid, C12 being a candidate for an apical substituent and the N5···P1 interaction completing the other apical substituent, as a "secondary" bond.[11] If it is so, it could be interpreted as a final stage in the opening of the central four-membered ring of **5**,[12,13] the situation being quite similar in the three structures.

(11) Burgi, H. B.; Dunitz, J. D. *Acc. Chem. Res.* **1983**, *16*, 153.
(12) Allcock, H. R. *Chem. Rev.* **1972**, *72*, 319.
(13) Smith, J. H. In *Comprehensive Organic Chemistry*; Barton, D., Ollis, W. D., Eds.; Pergamon: Oxford, 1979; Vol. 2, p 1233.

Table IV. Selected Dihedral Values (deg)

	3a·C	3a·D	3c
P1–N2–C3–N5	−0.4 (4)	2.5 (5)	−8.7 (10)
N2–C3–N4–N25	177.9 (3)	174.1 (4)	171.9 (8)
N2–C3–N5–C35	170.2 (3)	164.7 (4)	161.6 (7)
C3–N2–P1–C6	−65.1 (3)	−66.4 (4)	−42.9 (8)
C3–N2–P1–C12	−177.3 (3)	−179.0 (3)	−159.8 (7)
C3–N2–P1–C18	67.0 (3)	64.5 (4)	84.7 (8)
C24–N2–P1–C6	122.4 (3)	122.6 (4)	155.1 (7)
C24–N2–P1–C12	10.2 (3)	9.9 (4)	38.2 (8)
C24–N2–P1–C18	−105.6 (3)	−106.6 (4)	−77.3 (7)
P1–N2–C3–N4	179.1 (2)	−177.9 (3)	170.6 (6)
N4–C3–N2–C24	−8.0 (4)	−6.4 (6)	−27.1 (11)
N5–C3–N2–C24	172.5 (3)	174.1 (4)	153.5 (8)
N2–P1–C6–C7	−169.7 (3)	−173.4 (4)	139.2 (10)
N2–P1–C12–C13	−110.8 (3)	−111.4 (5)	−84.8 (10)
N2–P1–C18–C19	−139.3 (3)	−135.0 (4)	−20.6 (9)
C3–N4–N25–C26	128.1 (4)	133.7 (5)	144.3 (9)
C3–N5–N35–C36	130.2 (3)	134.1 (5)	143.5 (9)
N35–C36–S41–C42	178.0 (3)	173.9 (5)	−176.6 (9)
N25–C26–S31–C32	−179.2 (3)	173.5 (4)	172.9 (8)
N2–C24–C24A–C24B			−178.1 (9)
P1–N2–C24–C24A			−103.6 (9)
P1–N2–C24–H24A			11 (5)
P1–N2–C24–H24B			132 (8)

[N4–C3–N5] Anion. The N2, C3, N4, and N5 set of atoms is also planar. The opening of the N4–C3–N5 angle [139.7 (3), 138.5 (5), 138.2 (9)°] and the similar lengths of the C3–N5 and C3–N4 bonds [1.312 (4)–1.332 (6) Å] indicate a resonant character of this part of the molecule, which bears the negative charge, the positive one being localized in the P1–N2 part. With this situation, the C3–N2 lengths [from 1.427 (6) to 1.431 (4) Å] would give quite single character to the bond and, consequently, the possibility of the above-mentioned free rotation.

P1–N2 Cation. The P1–N2 lengths, 1.662 (3), 1.656 (4), and 1.651 (8) Å in **3a**·C, **3a**·D, and **3c**, respectively, are shorter than the usually assumed single-bond value of 1.77 Å,[12,14] suggesting some double-bond character (say 28%),[14] that supports, again, the pyramidality of P1, typical of equatorial P–N bonds in phosphorus with trigonal–bipyramid geometry.[13,14]

The N2 atoms present different planarity, the angles around it adding up to 359.6 (4), 359.0 (6), and 357.6 (11)°. **3c** presents a different overall conformation, in particular its Ph groups (see Figure 2). These facts lead us to study the distribution of the torsion angles around P1–N2 (see Table IV) as follows.

Deformations around the P1–N2 Bond. The Newman projections along this bond (see Figure 2) reveal two conformations resembling the two idealized forms of Allinger and Tribble,[15] the "parallel" one (∥), with 3–P–N–6 = 0° and 3–P–N–7 = 180°, and the "perpendicular" one (⊥), with 3–P–N–6 = 30° and 3–P–N–7 = 210°, the dihedral angles N–P–*i* (*i* = 3–5) being 120°.

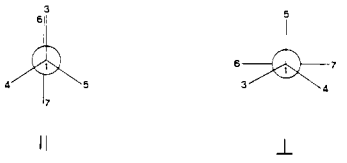

∥ ⊥

Compound **3a** (in both crystals, **3a**·C and **3a**·D) has, approximately, the parallel conformation, whereas **3c** crystallizes with a near-perpendicular one. So, this might be an indication that the energies of both conformers are quite similar, i.e. that the p_π–d_π overlapping is, to some extent, independent of the conformation. More striking seems to be the fact that the N2 hybridization is related to the conformation, as in the near-parallel one, of **3a**, N2 is sp^2, whereas in **3c**, with the quasi-perpendicular one, the distortion of the geometry around N2, as measured by the dihedral angle P–N–6 ∧ P–N–7 ≠ 180°, seems to indicate some sp^3 character. A similar situation for ylides was reported by Bart.[16] The observed situation (the parallel conformation having a P–X bond with more double-bond character than the perpendicular one) shows some similarity with the case of amides where a rotation about the C–N bond results in a lengthening of the C–N bond and in a pyramidalization of the N atom.[17]

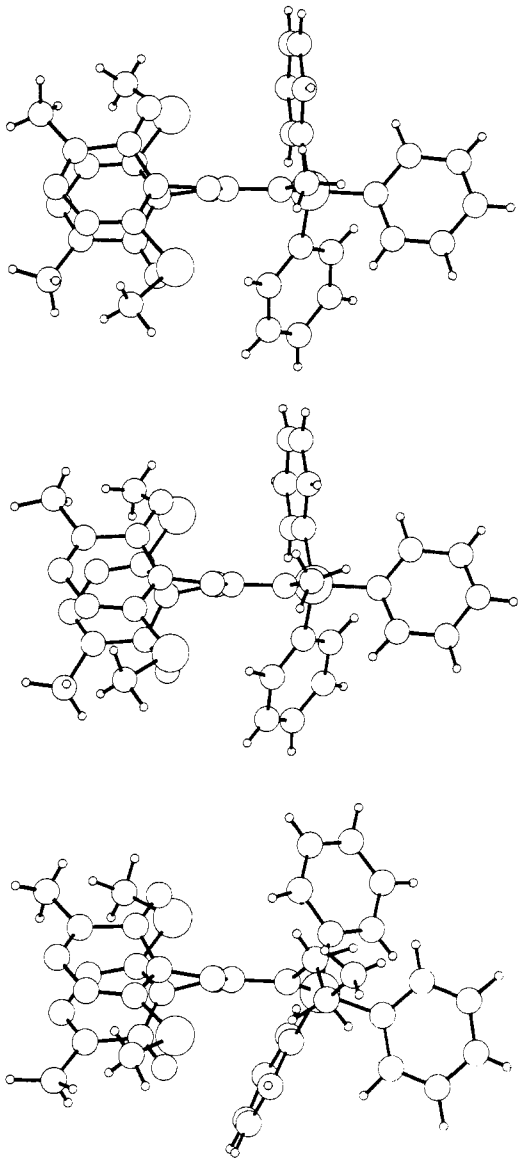

Figure 2. Newman projections along the P1–N2 bond for compounds **3a**·C, **3a**·D, and **3c**.

To study this effect, we searched the Cambridge data base[5] with a frame formed by a P attached to one N and to three C atoms and, then, the N atom linked to two non-hydrogen or metal ones. Rather surprisingly, only three hits **6**,[18] **7**,[19] and **8**[14] matched the requirement and, even, two of them, **6** and **7**, have as N-substituents Si and Ge, respectively, but their similarity with the C species made them acceptable.

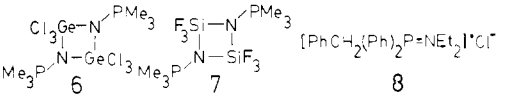

6 7 8

(14) Bart, J. C.; Bassi, I. W.; Calcaterra, M. *Acta Crystallogr.* **1982**, *B38*, 1932.
(15) Allinger, N. L.; Tribble, M. T. *Tetrahedron Lett.* **1971**, 3259.
(16) Bart, J. C. *J. Chem. Soc. B* **1969**, 350.
(17) Cieplak, A. S. *J. Am. Chem. Soc.* **1985**, *107*, 271 and references therein.
(18) Sheldrick, W. S.; Wolfsberger, W. *Z. Naturforsch., B: Anorg. Chem., Org. Chem.* **1977**, *32*, 22.
(19) Sheldrick, W. S.; Schomburg, D.; Wolfsberger, W. *Z. Naturforsch., B: Anorg. Chem., Org. Chem.* **1978**, *33*, 493.

Table V. Deformations (deg) around the P→N$^{\delta+}$ Bond in Compounds **3a**·C, **3a**·D, **3c**, **6**, **7**, and **8**

compd	atom type[a] 3	4	5	6	7	χ_{34}[b]	χ_{53}	χ_{45}	χ_{67}[c]	φ (180 − χ_{67})	χ_τ[d]	$\sum\hat{N}_{obs}$[e]	$\sum\hat{N}_{calc}$[f]
3a·C	C12	C6	C18	C24	C3	−7.8	−4.2	12.0	7.5	172.5	5.3	359.6	359.6
3a·D	C12	C6	C18	C24	C3	−7.3	−3.5	10.8	8.9	171.1	4.2	359.4	359.4
3c	C12	C6	C18	C24	C3	−3.1	−4.5	7.6	18.0	162.0	29.7	357.6	357.5
6	C	C	C	Ge	Ge	−3.5	−2.6	6.1	1.3	178.7	−0.2	360.0	360.0
7	C	C	C	Si	Si	−1.1	−0.8	1.9	4.4	175.6	3.2	359.9	359.9
8	C	C	C	C	C	−2.8	−2.7	5.5	30.1	171.4	8.6	353.6	352.9

[a] See scheme of the Newman projection. [b] χ_{ij} measures the deviation, from the ideal value, of the dihedral angle between two planes with common edge at the P–N bond. The negative sign indicates that when we go anticlockwise, from *i* to *j*, and view from the PH_3 end, the dihedral angle is less than the ideal one. For changes in the viewing or in the order of sustituents, just reverse the sign. [c] χ_{67} (or φ) is a measure of the pyramidalization of the N2 atom. [d] χ_τ follows the same criteria as the usual torsion angles. It measures the twist of the rear-end substituents with respect to the front end ones, corrected for deformation and from an ideal position that here has been chosen as the one eclipsing substituents 3 and 6. [e] Pyramidalization may also be described by the sum of bond angles around N2. [f] This sum $\sum\hat{N}_{obs}$, can be estimated approximately from the φ value by the spherical trigonometric relationship 2 sin (φ/2) cos [$\sum\hat{N}_{calc}$/6] = 1.

Table VI. 6-31G* Energies, Dipole Moments, Mulliken Total Atomic Populations, and Mulliken Overlap Populations of P–X Bonds for Compounds **9**–**12d**

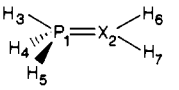

compd		conformn	*E*, au	ΔE, kcal·mol^{-1}	μ, D	X2	P1	H3	H4	H5	H6	H7	*c*
H_3PO	**9**		−417.306 807		4.17	8.718	14.077	1.069	1.069	1.069			0.556
H_3PNH	**10a**	∥ H eclipsed	−397.423 917	2.13	3.41	7.941	14.227	1.068	1.058	1.058	0.647		0.598
	10a′	∥ H anti	−397.427 310	0	3.37	7.918	14.242	1.020	1.080	1.080		0.659	0.593
	11a	∥	−397.820 272	0.28		7.994	14.154	0.915	0.930	0.930	0.537	0.541	0.396
$[H_3PNH_2]^+$	**11b**	*a*	−397.820 384	0.21		7.993+	14.155	0.915	0.923	0.936	0.538	0.541	0.395
	11c	*b*	−397.820 623	0.06		7.987	14.158	0.914	0.917	0.941	0.540	0.542	0.394
	11d	⊥	−397.820 712	0		7.983	14.161	0.915	0.915	0.942	0.542	0.542	0.393
H_3PCH_2	**12a**	∥	−381.390 750	1.00	2.43	6.811	14.425	1.005	1.066	1.066	0.809	0.818	0.607
	12d	⊥	−381.392 338	0	2.48	6.779	14.438	1.017	1.017	1.102	0.824	0.824	0.627

[a,b] Intermediate conformations, see Table X in the supplementary material and Figure 6. [c] Overlap populations of P–X bonds.

Table VII. Selected Geometrical Parameters of Compounds **9**–**12d** (Bonds, Å; Angles, deg) Corresponding to 6-31G* Calculations[a]

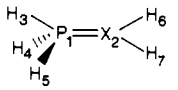

compd	PX	∠6213	∠6214	∠6215	∠7213	∠7214	∠7215
9	1.465						
10a	1.543	0	121.6	−121.6			
10a′	1.548				−180.6	−62.9	61.6
11a	1.621	0	119.2	−119.2	−180.0	−60.8	60.8
11b	1.621	15.0	134.2	−104.4	−172.5	−53.3	68.1
11c	1.623	30.0	148.8	−90.1	−167.4	−48.6	72.5
11d	1.624	41.7	160.2	−79.1	−160.2	−41.7	79.0
12a	1.655	0	118.6	−118.6	−180.0	−61.4	61.4
12d	1.667	45.6	163.3	−75.6	−163.3	−45.6	75.6

[a] Bond lengths and bond angles involving hydrogen atoms (PH, XH, ∠HPH, and ∠HXH) are to be found in the supplementary material.

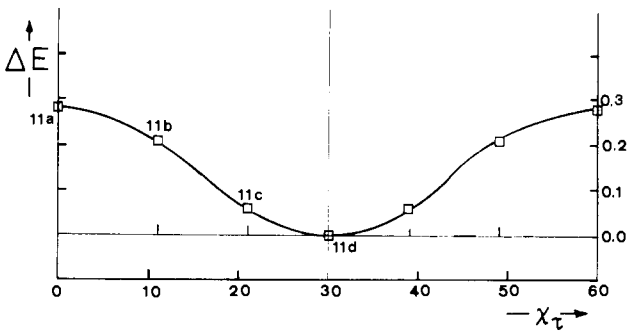

Figure 3. Energy profile (in kcal·mol^{-1}) of the rotation about the N2–P1 bond in compound **11**.

The deformation from the ideal parallel shape of the substituents in the P1–N2 bond in components **3a**·C, **3a**·D, 3c, **6**, **7**, and **8** has been analyzed by means of the torsion angles around the bond.[20] The results of this analysis appear in Table VIII. It can be noticed that the dihedral angle N–P–4 ∧ N–P–5 is always opened (as measured by χ_{45}) at the expense of the other two, being closed. It is also apparent that the staggering–pyramidalization relationship holds quite regularly ($\varphi - \chi_\tau$) except for **8**, which is largely distorted (30.1°) in relation with the achieved staggering of 8.6°.

Spectroscopy. It is convenient to discuss the NMR results of Table II on the basis of the solid-state molecular structures **3a** and **3c**.

Cyclic structure **5** can be ruled out in solution since (i) the ^{31}P chemical shifts are incompatible wiith a pentacoordinated phosphorus,[21–23] and (ii) only one heterocyclic residue is observed both in ^1H and ^{13}C NMR. This means thhat there is a free rotation about the C3–N2 bond in **3**. To concilitate the fact that methylene protons are diastereotopic with the fact that only one kind of phenyl is observed, we must assume that there is an intrinsic chirality at the phosphorus but that a rapid pseudorotation mechanism is exchanging the phenyl residues *without destroying the chirality*. The thermal fragility of these betaines prevents high-temperature NMR studies in order to determine the origin (intrinsic and conformational) of the observed anisochrony.

Assuming that the conformation of the N residue in **3b** and

(20) Cano, F. H.; Foces-Foces, C.; Garcia-Blanco, S. *J. Cryst. Mol. Struct.* **1979**, *9*, 107.

(21) Mavel, G. In *Annual Reports on NMR Spectroscopy*; Mooney, E. F., Ed.: Academic: New York, 1973: Vol. 5B, pp 33, 44. Verkade, J. G.; Quin, L. D. *Phosphorus-31 NMR Spectroscopy in Stereochemical Analysis*; VCH: Dearfield Beach, FL, 1987.

(22) Albright, T. A.; Freeman, W. J.; Schweizer, E. E. *J. Org. Chem.* **1976**, *41*, 2716.

(23) Maryanoff, B. E.; Reitz, A. B.; Muller, M. S.; Inners, R. R.; Almond, H. R.; Whittle, R. R.; Olofson, R. A. *J. Am. Chem. Soc.* **1986**, *108*, 7664.

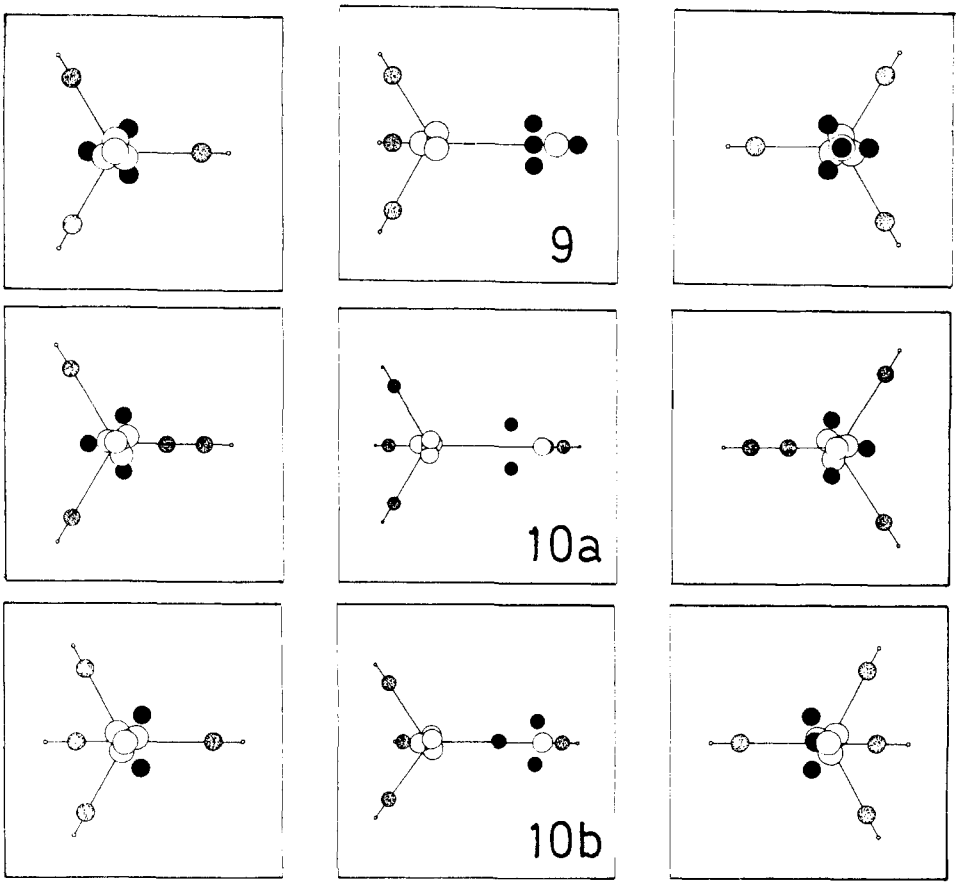

Figure 4. Centroids of molecules **9**–**10b** viewed in lateral and Newman projections.

Table VIII. Deformations around P⁻⁻X in Compounds **11a**–**12d**[a]

compd	conformn		χ_{34}	χ_{53}	χ_{45}	χ_{67}	φ (180 − χ_{67})	χ_τ	$\sum\hat{X}_{obs}$	$\sum\hat{X}_{calc}$
$[H_3PNH_2]^+$	**11a**	∥	−0.8	−0.8	1.6	0	180	0	360	360
	11b	*b*	−0.8	−0.6	1.4	7.5	172.5	11.2	359.6	359.5
	11c	*c*	−1.2	0.1	1.1	17.4	162.6	20.9	357.9	357.7
	11d	⊥	−1.5	0.7	0.8	21.9	158.1	30.0	356.6	356.3
H_3PCH_2	**12a**	∥	−1.4	−1.4	2.8	0	180	0	360	360
	12d	⊥	−2.3	1.1	1.2	28.9	151.1	30.0	353.3	353.5

[a] The parameters shown in the table have the same meaning as those in Table V. [b,c] Intermediate conformations; see Figure 6.

3c is the same, the coupling constants of these two compounds are in agreement with the structure determined by X-ray.

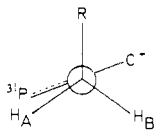

$H_ANCP = 11°$, $^3J \simeq 14.0$ Hz
$H_BNCP = 132°$, $^3J \simeq 17.0$ Hz
3b, R = Me; **3c**, R = Et

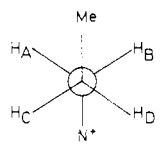

J_{AC} and J_{BD}: J_{gauche}
J_{AD} and J_{BC}: J_{trans}
3c

The $^3J(^1H-^{31}P)$ coupling constants (mean values) follow a Karplus-type curve for these kinds of vicinal couplings. The $^1H-^1H$ coupling constants of the CH_2-CH_2 fragment in compound **3c** correspond to a classical staggered conformation. Finally, the low-frequency resonance of the methyl group (0.64 ppm) in compound **3c** results in its proximity to the phenyl groups (see Figure 2c).

Theoretical Calculations

In Description of Structures dealing wiith the λ^5-phosphiniminium part (Table V), we have stressed that two types of molecular structures are found in solid state:

$[R_3P{=}NX_2]^+$ { ∥: $\tau = 0°$, $\varphi = 180°$ (**3a**•C, **3a**•D, **6**, **7**: $\bar{\tau} = 3.1°$, $\bar{\varphi} = 175.0°$)
⊥: $\tau = 30°$, $\varphi = 160°$ (**3c**, $\tau = 29.7°$, $\varphi = 162.0°$)

In order to provide a theoretical ground to this observation, quantum mechanical calculations have been carried out on H_3PO, H_3PNH, $[H_3PNH_2]^+$, and H_3PCH_2 at the 6-31G* level.[24,25] The geometries were fully optimized following a suitable gradient procedure[29] using an IBM version of the GAUSSIAN 80 series of programs[30] at the UAM/IBM Scientific Center, Madrid.

Table VI contains 6-31G* energies, dipole moments, Mulliken total atomic populations, and Mulliken overlap populations off the P–X bond for the four compounds: **9**, **10** (**a**, H eclipsed; **a'**, H anti), **11** (four conformations), and **12** (**a**, parallel; **d**, perpendicular). In the case of **10**, the most stable of the parallel conformations is the anti one, **10a'** (Figure 6). A CNDO/2 calcu-

(24) Francl, M. M.; Pietro, W. J.; Hehre, W. J.; Binkley, J. S.; Gordon, M. S.; De Frees, D. J.; Pople, J. A. *J. Chem. Phys.* **1982**, *77*, 3654 and references therein.

(25) We have also carried out STO-3G* calculations[26] to have an initial geometry for the 6-31G* calculations. As it has been reported in the literature[27] and as we have shown ourselves,[28] the explicit inclusion of d orbitals is necessary to obtain a meaningful description of hypervalent structures.

(26) Collins, J. B.; Schleyer, P. R.; Binkley, J. S.; Pople, J. A. *J. Chem. Phys.* **1976**, *64*, 5142.

(27) Hehre, W. J.; Radom, L.; Schleyer, P. R.; Pople, J. A. *Ab Initio Molecular Orbital Theory*; Wiley: New York, 1986.

(28) Catalán, J.; De Paz, J. L. G.; Elguero, J.; Rozas, I., accepted for publication in *THEOCHEM*.

(29) Murtagh, B. A.; Sargent, R. W. H. *Comput. J.* **1982**, *131*, 185. Schelegel, H. B. *J. Comput. Chem.* **1982**, *3*, 214.

(30) Binkley, J. S.; Whiteside, R. A.; Krishnan, R.; Seeger, R.; De Frees, D. J.; Schlegel, H. B.; Topiol, S.; Kahn, L. R.; Pople, J. A. Program GAUSSIAN 80, Department of Chemistry, Carnegie-Mellon University, IBM version by E. M. Fluder and L. R. Kahn.

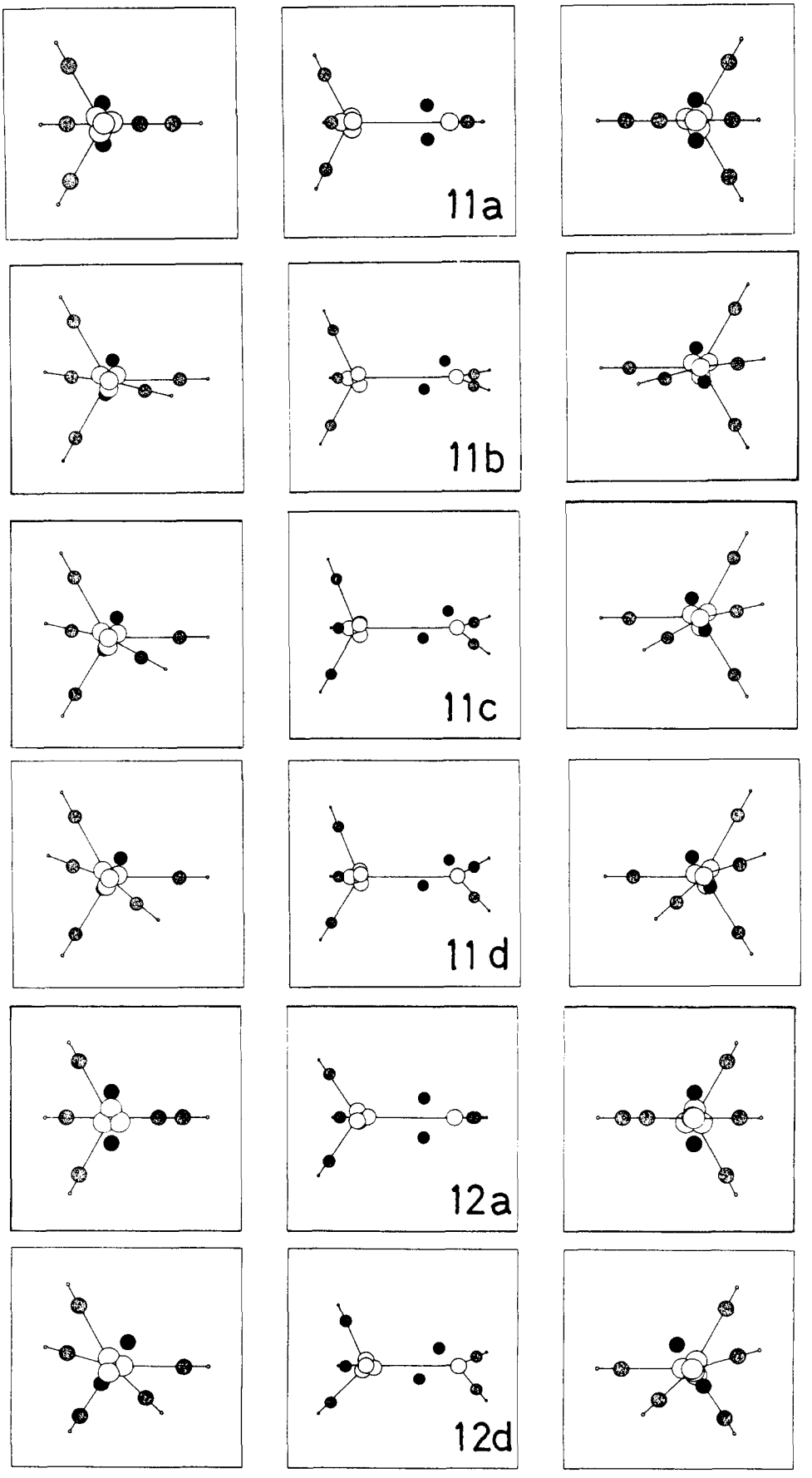

Figure 5. Centroids of molecules **11a–12d** viewed in lateral and Newman projections.

lation[31] on Me_3PNH afforded similar results ($\Delta E \sim 1$ kcal·mol^{-1}). For compounds **11** and **12** perpendicular conformations are more stable than parallel ones, but the differences in energy are so small that for practical purposes there is free rotation about the P–X bond.

In the case of the salt of λ^5-phosphiniminium, two intermediate

conformations have been calculated. The variation of the energy with the torsion angle χ_τ (see later) is represented in Figure 3.

Tables VII and VIII include all the relevant geometrical information, the last one having a similar structure as Table V. Taking into account the different substituents, the P–X distance is in good agreement with the experimental bond lengths, compare **9** and triphenylphosphine oxide (d(PO) = 1.462–1.484 Å),[5] **10** and [(*p*-bromophenyl)imino]triphenylphosphorane (d(PN) = 1.567 Å),[32] **11** and Table III (d(PN) = 1.656 Å), and **12** and methylenetriphenylphosphorane (d = 1.661 Å).[16] Other distances and angles involving hydrogen atoms are difficult to compare, except between **12a** (H_3PCH_2, ‖), $d(CH_6) = d(CH_7)$ = 1.072 Å, ∠512 = 121.6°, ∠621 = 118.1°, and ∠721 = 122.0°, and methylenetriphenylphosphorane (Ph_3PCH_2, ‖),[16] $d(CH_6) = d(CH_7)$ = 1.01 Å, ∠512 = 120.8°, ∠621 = 113.2°, and ∠721 = 124.2°.

Table VIII shows that two limit situations are found for compounds **11** and **12**: the parallel, $\chi_\tau = 0$, $\varphi = 180°$, and the perpendicular, $\chi_\tau = 30$, $\varphi = 155°$, in quite good agreement with the results of Table V for compound **11** and Ph_3PCH_2 ‖ (χ_τ = 0, $\varphi = 180°$) for compound **12a**. This is one of the main conclusions of this work: similar to what occurs in amides,[17] rotation about the central bond is accompanied by pyramidalization of the X atom (X=N^+ or C); however, in the case of the P=X bond, the energy is rather insensitive to conformational changes. This means that, in spite of pyrimidalization upon rotation, the doouble bond remains. A possible explanation is that, as the π bonds are formed between p orbitals of X and d orbitals of P, the overlapping between both orbitals can remain almost constant during rotation. The approximately constant Mulliken overlap populations for the P=N bond and the low change for the P=C bond are consistent with the above explanation.

In order to obtain a visual description of these molecules, we have calculated, with the Foster and Boys procedure,[33] the localized molecular orbitals. When the PLUTO package is used,[5] Figures 4 and 5 have been drawn, small circles corresponding to hydrogen atoms. Three kinds of centroids are represented: large ones correspond to phosphorus, medium-dotted ones to P–H and X–H bonds, and medium black circles to the P–X bond.

The Newman projections along the P–N bond for the four conformations **11a–11d** are represented in Figure 6 and correspond to the energy profile of Figure 3. The PH_3 group serves as reference. The increasing NH pyrimidalization on going from **11a** to **11d** is clearly apparent. The centroids corresponding to the P–H bonds slightly deviate from the line joining both atoms.

All the molecules in parallel and perpendicular conformations viewed in three projections, a lateral view and two standard Newman projections viewed from the phosphorus (left side) and from the X atom (right side), are represented in Figures 4 and 5. Phosphine oxide **9** has a very peculiar electronic distribution: there is neither a centroid along the P–O bond, as it would be expected for an ylide H_3P^+–O^-, nor the two centroids of the double bond of H_3P=O. The Newman projections show the "staggered" conformation of three centroids, the fourth one being situated in the P–O direction.

The effect of the basis sets on H_3PO geometry has been discussed by Bollinger et all.[34] and by Streitwieser et all.[35] In order to obtain results comparable with our 6-31G* calculation (Table VII), it is necessary to use the double-ζ basis set of Dunning plus d AO on phosphorus[34] or basis sets of at least split-valence shell quality with d orbitals on all heavy centers.[35]

On the basis of qualitative considerations, Singleton[36] concludes that the P–O bond has a triple-bond character. Kutzelnigg[37] considers that neither the H_3P^+–O^- nor the H_3P=O formula is

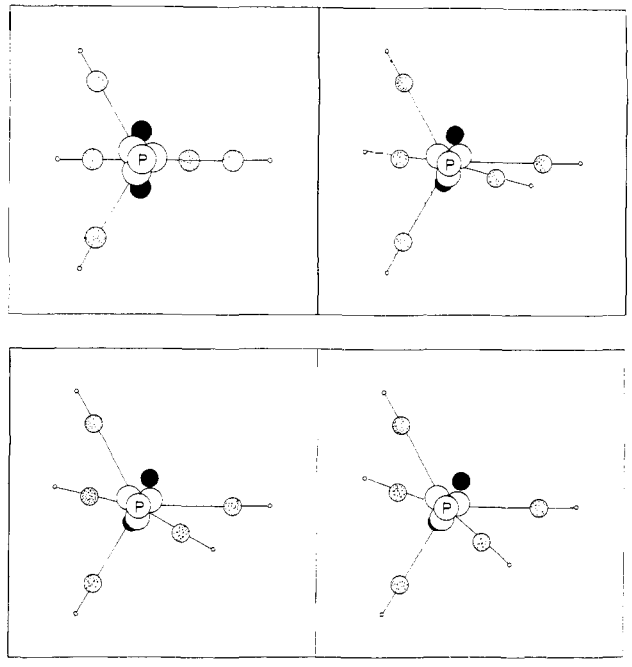

Figure 6. Newman projections along the P–N bond for conformations **11a–11d** corresponding to Figure 3.

appropriate to describe H_3PO and that it woould be more justified to refer to a partial triple bond. According to Streitwieser et al.,[35] "the dipolar structure H_3P^+–O^- dominates in phosphine oxide and the double-bond structure H_3P=O contributes but little".

The Foster and Boys LMO picture (Figure 4 and 5) describes the P–O bond in phosphine oxide as a triple bond. To check if this is not an artifact, we have carried out 6-31G* calculations on H_3NX (X = O, NH, and CH_2).[38] In these cases, the LMO's show an N–X single bond (one centroid along the N–X bond and the remaining ones around the X group). On the other hand, the LMO's of H_3PO have been calculated with the following basis sets: STO-3G, STO-3G*, 6-31G, 6-31G*, 6-31G plus one set of d functions on P, 6-31G plus two sets of d functions on P, one set of d functions on O, one set of p functions on H (6-31G** + dp), and 6-31G plus BF(P–O) exp 0.5. All these basis sets, which include d functions on P or BF(P–O), yield an LMO picture corresponding to a triple bond between P and O. The basis sets without polarization on P yield a single-bond structure (P–O).

The large negative charge on the oxygen, which other authors[35,37] have also found, is in our opinion consistent with the triple-bond chharacter of the P–O bond. The difference in electronegativity (oxygen, 3.5; phosphorus, 2.1)[39] leads to a peculiar triple bond whose three LMO's (Figures 4 and 5) are clearly shifted toward the oxygen. As a consequence of the Mulliken analysis, the gross atomic population on the oxygen, 8.817 (Table VI) (Kutzelnigg[37] found 8.97), underestimates the true charge of this atom (Streitwieser et al.[35] reported an integrated oxygen charge of −1.53 to −1.58). In conclusion, phosphine oxide should be represented as $H_3P^+\equiv O^-$.

The two parallel conformations, **10a** and **10a′**, of the iminophosphorane (λ^5-phosphinimine) have very similar centroids: both have one along the P–N bond (slightly bent) and two other centroids on the nitrogen. This corresponds to an ylide structure H_3P^+–N^-H.

The N-protonation of the iminophosphorane **10** leads to the salt **11**, which has been named iminium phosphorane (H_3P=N^+H_2) or aminophosphonium (H_3P^+–NH_2). The centroids represented in Figures 4 and 5 are very similar in the parallel and perpendicular conformations and show the existence of a double

(31) Ostoja-Starzewski, K. A., Dieck, H. T. *Inorg. Chem.* **1979**, *18*, 3307.
(32) Hewlins, M. J. E. *J. Chem. Soc. B* **1971**, 942.
(33) Boys, S. H. In *Quantum Theory of Atoms, Molecules and Solid State*; Lowdin, P. O., Ed.; Academic: New York, 1966; p 253.
(34) Bollinger, J. C.; Houriet, R.; Kern, C. W.; Perret, D.; Weber, J.; Yvernault, T. *J. Am. Chem. Soc.* **1985**, *107*, 5352.
(35) Streitwieser, A.; Rajca, A.; McDowell, R. S.; Glaser, R. *J. Am. Chem. Soc.* **1987**, *109*, 4184 and references therein.
(36) Singleton, R. *J. Chem. Educ.* **1973**, *50*, 538.
(37) Kutzelnigg, W. *Angew. Chem., Int. Ed. Engl.* **1984**, *23*, 272.
(38) Catalán, J.; De Paz, J. L. G.; Foces-Foces, C.; Cano, F. H.; Elguero, J., to be published in *THEOCHEM*.
(39) Pauling, L. *The Nature of the Chemical Bond*, 3d ed.; Cornell University: Ithaca, NY, 1960; p 94.

bond. The pyrimidalization of the nitrogen in **11d** (due to torsion) does not destroy the double-bond character of the P–N bond. The P–N bond length slightly increases by protonation (**10** → **11**) as a consequence of a small charge redistribution.

Finally, the case of methylenephosphorane **12** is quite similar to the preceding one. The compound is better represented as $H_3P{=}CH_2$ than as $H_3P^+{-}C^-H_2$. The centroids corresponding to the double bond are further apart and nearer the phosphorus in **12a** than in **11a** as expected from the corresponding X electronegativities (nitrogen, 3.0; carbon, 2.5).[39] Conformation **12d** shows a bent CH_2 and a distorted double bond (the centroid opposed to H_5 is near the phosphorus). The structure corresponds to the description of $Ph_3P{=}CH_2$ (on the contrary, the arsonium analogue is better represented as $Ph_3As^+{-}CH_2^-$).[40]

The most stable structure of methylenephosphorane, **12d**, has been calculated recently by high-level methods. With basis sets like double-ζ augmented with d functions on phosphorus, 6-31G*,[42] or 3-21G*,[35] the optimized geometries are almost identical with those of Table X of the supplementary material (e.g. d(PO) = 1.667 ± 0.001 Å). Better basis sets, 3-21+G*,[35] and MP/2-6-31G*[42] yield slightly different geometries (e.g. d(PO) = 1.675 ± 0.002 Å). The GVB orbitals of **12d** have been discussed by Dixon et all.:[41] they are similar to the LMO's obtained with the Foster and Boys criterion. When the present publication was in press, a theoretical study of methylenephosphorane and related compounds appeared.[43]

(40) Lloyd, D.; Gosney, I.; Ormiston, R. A. *Chem. Soc. Rev.* **1987**, *16*, 45.
(41) Dixon, D. A.; Dunning, T. H.; Eades, R. A.; Gassman, P. G. *J. Am. Chem. Soc.* **1983**, *105*, 7011 and references therein.
(42) Yates, B. F.; Bouma, W. J.; Radom, L. *J. Am. Chem. Soc.* **1987**, *109*, 2250 and references therein.

Conclusions

In this paper, we have presented experimental and theoretical evidence of a new class of compounds, the pseudocyclic betaines derived from λ^5-phosphiniminium salts. Consistent with experimental observations, theory confirms that rotation about the P–N bond results in changes of the nitrogen pyrimidalization.

Registry No. 1, 109107-00-8; **3a**, 117369-71-8; **3a**·C, 117369-74-1; **3a**·D, 117407-39-3; **3b**, 117369-73-0; **3c**, 117369-72-9; **3c**·2CHCl$_3$, 117369-75-2; **4d**, 117342-08-2; **6**, 42584-20-3; **7**, 33378-27-7; **8** (isomer1), 82861-54-9; **8** (isomer2), 82857-68-9; **9**, 13840-40-9; **10**, 61559-67-9; **11**, 88392-38-5; **12**, 36429-11-5; MeNCO, 624-83-9; EtNCO, 109-90-0; *n*-PrNCO, 110-78-1; *t*-BuNCO, 1609-86-5.

Supplementary Material Available: Tables of anisotropic thermal parameters, atomic parameters, interatomic distances and angles, and 6-31G* calculated geometries of compounds **9–12d** (52 pages); listings of observed annd calculated structure factors (77 pages). Ordering information is given on any current masthead page.

(43) Francl, M. M.; Pellow, R. C.; Allen, L. C. *J. Am. Chem. Soc.* **1988**, *110*, 3723.

Communications to the Editor

Sequence-Specific ^{13}C NMR Assignment of Nonprotonated Carbons in $[d(TAGCGCTA)]_2$ Using Proton Detection

Joseph Ashcroft,[1a] Steven R. LaPlante,[1b] Philip N. Borer,[1b] and David Cowburn*[,1a]

The Rockefeller University, 1230 York Avenue New York, New York 10021
NMR and Data Processing Laboratory NIH Resource, Syracuse University Syracuse, New York 13244-1200
Received July 25, 1988

Carbon-13 NMR assignments of protonated carbons can be made by using proton-detected heteronuclear correlation spectroscopy, and this experiment has been applied to DNA oligomers.[2-5] The multibond coupling optimized heteronuclear multispin coherence proton-detected COSY (MC-HMP-COSY) NMR experiment supplies the correlation between ^{13}C's and protons that are not directly bonded, but are coupled. This experiment has been applied to vitamin B_{12},[6,7] a peptide,[8] trisaccharides,[9] and a polysaccharide with a single repeating monomeric unit,[10] and experimental details are covered in the above cited references.

This communication describes the MC-HMP-COSY experiment applied to the assignments of the nonprotonated carbons

Table I. ^{13}C Chemical Shifts of Nonprotonated Carbons in $[d(TAGCGCTA)]_2$

assignment/pathway (proton/carbon)	1-D ^{13}C chemical shift (ppm)	MC-HMP-COSY ^{13}C chemical shift (ppm)
G3(H8|C4)	153.41[a-c]	153.4
G3(H8|C5)	117.49[b,c]	117.8
G5(H8|C4)	153.73[a-c]	153.6
G5(H8|C5)	117.79[b,c]	118.2
C4(H6|C2)	158.95[b]	159.3
C4(H6|C4)	168.12[b]	168.1
C6(H6|C2)	158.95[b]	159.2
C6(H6|C4)	168.25[b]	168.3
A2(H2|C4)	151.18[b]	151.3
A2(H8|C5)	120.88[b]	120.8
A2(H2|C6)	158.30[b]	158.3
A8(H2|C4)	151.18[b]	151.25
A8(H8|C5)	120.81[b]	120.8
A8(H2|C6)	158.11[b]	158.2
T1(H6|C2)	153.73[a-c]	153.7
T1(Me or H6|C4)	168.83[c]	169.0
T1(Me|C5)	113.87[c]	114.1
T7(H6|C2)	153.41[a-c]	153.5
T7(Me or H6|C4)	169.37[c]	169.4
T7(Me|C5)	113.57[c]	113.8

[a] Distinction of GC4 and TC2 was ambiguous in the 1D study.[3,11] [b] Assignments within a carbon class were not clear in the 1D study.[3,11] [c] Unambiguous assignments made according to MC-HMP-COSY.

(1) (a) The Rockefeller University. (b) Syracuse University. J.A.'s current address: Lederle Laboratories, Pearl River, New York.
(2) LaPlante, S. R.; Ashcroft, J.; Cowburn, D.; Levy, G. C.; Borer, P. N. *J. Biomol. Str. Dyn.* **1988**, *5*, 1089-1099.
(3) LaPlante, S. R.; Boudreau, E. A. Zanatta, N.; Levy, G. C.; Borer, P. N.; Ashcroft, J.; Cowburn, D. *Biochemistry* **1988**, *27*, 7902-7909.
(4) Leupin, W.; Wagner, G.; Denny, W. A.; Wüthrich, K. *Nucl. Acids Res.* **1987**, *15*, 267-275.
(5) Sklenar, V.; Bax, A. *J. Am. Chem. Soc.* **1987**, *109*, 2221-2222.
(6) (a) Bax, A; Summers, M. F. *J. Am. Chem. Soc.* **1986**, *108*, 2093-4. (b) Summers, M. F.; Marzilli, L. G.; Bax, A. *J. Am. Chem. Soc.* **1986**, *108*, 4285-94.
(7) Bax, A.; Marzilli, L. G.; Summers, M. F. *J. Am. Chem. Soc.* **1987**, *109*, 566-574.
(8) Bermel, W.; Griesinger, C.; Kessler, H.; Wagner, K. *Magn. Reson. Chem.* **1987**, *25*, 325-326.
(9) Lerner, L.; Bax, A. *Carbohydr. Res.* **1987**, *166*, 35-46.
(10) Byrd, R. A.; Egan, W.; Summers, M. F. *Carbohydr. Res.* **1987**, *166*, 47-58.

0002-7863/89/1511-0363$01.50/0